Radiative energy release quantification of subsurface coal fires

C. Fischer [a],*, J. Li [b], C. Ehrler[a], J. Wu [b]

[a] German Aerospace Center, German Remote Sensing Data Center, Dept. Land Surface, Oberpfaffenhofen, Germany – (c.fischer, christoph.ehrler)@dlr.de
[b] Beijing Normal University, Academy of Disaster Reduction and Emergency Management, Beijing, P.R. China – (lijing, wjj)@ires.cn

Abstract - Monitoring and calculation of coal fire radiative energy (CFRE) are an advanced field of application for satellite imagery. The five thermal infrared bands of the Advanced Spaceborne Thermal Emission and Reflection Radiometer (ASTER) proved to be suitable for automated fire pixel detection and energy release quantification. Two different automated algorithms were tested on night-time imagery. To improve the robustness of the detection and to reduce influences caused by solar radiation, which may lead to overestimating the energy release, the interest has been focussed on modelling the energy release from a subsurface fire and the fire related impacts on soil and surface temperatures. Discrepancies in CFRE estimations can be detected by comparing the results of satellite data analysis and modelling. This leads to a new validation possibility. A reliable quantification of CFRE is a valuable input for coal fire monitoring and may support green house gas emission estimations. The latter contributes to a coal fire related CDM methodology which is currently under development.

Keywords: coal fire, radiative energy quantification, energy balance, temperature modelling

1. INTRODUCTION

Coal seam fires are an environmental and economic problem of international magnitude. The spontaneous nature of coal fires makes them difficult to predict. While affecting a limited natural resource the fire causes disruption in the mining operations, irreversible loss of energy resources and release of toxicants transported by air and water polluting the environment.

China is today's world leading coal producer, consumer and exporter. Its coal producing industry faces the problem of more than 50 coal fields affected by uncontrolled burning coal seam fires. Comprehensive studies of the Sino-German Coal Fire Research Initiative focused on a better understanding of self-ignition, burning processes and monitoring aspects of spontaneous coal seam fires.

The determination of the fire radiative energy (FRE) has been introduced as a remote sensing technique to quantify forest and grassland fires. Various methods for fire detection and FRE quantification have been developed, which can be categorized into single-band algorithms and multi-band algorithms. Dozier (1981) introduced a widely used bi-spectral algorithm. It takes advantage of the non-linear nature of the Planck function to calculate fire temperature and fire size on a sub-pixel basis. This bi-spectral fire temperature and fire area can be used to estimate FRE (Wooster et al. 2003). In contrast Kaufman et al. (1998) and Wooster et al. (2003) use a single band algorithm to directly derive FRE of a sub-pixel fire component.

In opposite to burning vegetation fires, the coal fire radiative energy (CFRE) is comparably small as most fires are covered by bedrock. Tetzlaff (2004) conducted a sensitivity study on the ASTER, ETM+ and BIRD TIR satellite sensor systems and found ASTER and ETM+ suitable for energy release quantification using a single band method. The BIRD system facilitates the application of the Dozier method, but the spatial resolution of BIRD unfortunately has been proofed to be not adequate for the relatively small scale coal fire anomalies in some cases.

Single band methods rely on the robust demarcation of background pixels and fire influenced anomalous pixels. A long-term monitoring and CFRE quantification analysis on multiple temporal separated TIR scenes is feasible only when a reliable fire pixel identification independent from environmental factors can be guaranteed.

Investigations have been focused on modelling the energy release of the topographic surface. This was done based on the analysis of the surface energy balance incorporating analytical and numerical solutions for estimating the individual energy terms. The balancing model applies site-specific field data gathered throughout measuring campaigns and data from other remote sensing systems, e.g. MODIS products.

Field measurements (Schlömer, 2010) showed a significant part of the energy to be transported by exhaust gases and corresponding heat convection if a system of fissures and cracks does exist. This non-radiative part as well as all lateral energy fluxes can not be observed by remote sensing.

2. MULTITEMPORAL ANALYSIS

A monitoring attempt of coal fire radiative energy release (CFRE) was conducted for the site of Wuda (Inner Mongolia Province, P.R. China) using 9 ASTER night time TIR scenes of the year 2007. Automated detection of surface temperature anomalies in the atmospherically minor influenced ASTER TIR band 13 was done using the algorithm of Zhang (2004). It employs statistical methods using a moving window technique. On each move of the window a set of statistical tests is performed to identify potential coal fire related thermal anomalies in large areas. These tests include a histogram-based dynamic threshold and growing-window statistics for false alarm removal.

In order to work on standardized data for the CFRE retrieval and to convert raw digital numbers of the satellite image into physically meaningful values the ATCOR program (Richter, 1998) was used for atmospheric correction and ground leaving radiance calculation. As a critical correction parameter the water vapour column (WVC) of the atmosphere has a major impact on the quality of the atmospheric correction.

ASTER TIR band 10 was used to quantify the fire radiative energy of the anomaly pixels that were flagged by the detection

---

*   Corresponding author.

algorithm. Tetzlaff (2004) showed that ASTER TIR band 10 is sensitive in the coal fire emission range and it has the best correlation of fire radiative energy to the registered ground-leaving spectral radiance compared to the other ASTER thermal bands. The second order polynomial best-fit Relationship 1 was derived by Tetzlaff (2004) to set up an ASTER single band method applicable to the typical coal fire temperature range of 350 to 600 K. It computes the CFRE from the fire (L_{fire}) to background (L_{bg}) pixel radiance difference.

$$CFRE = a + b \cdot (L_{fire} - L_{bg}) + c \cdot (L_{fire} - L_{bg})^2 \qquad (1)$$

A second study of the Wuda test site using the same ASTER scenes is based on an adaptive threshold to separate coal fires from background pixels (Zhukov, 2010). The first-order Relationship 2 is used to calculate CFRE from at-sensor spectral radiance difference between fire pixels L_{fire*} and background L_{bg*} using ASTER TIR band 13. Though using at-sensor radiance the method corrects for emissivity and atmospheric effects on CFRE.

$$CFRE = d \cdot (L_{fire*} - L_{bg*}) \qquad (2)$$

3. ENERGY BALANCE MODELLING

An energy balance model of the topographic surface was implemented consisting of three linked parts, which are (i) attenuation of solar irradiation in the atmosphere, (ii) energy conversion at the surface and (iii) dissemination of temperature in the subsurface.

A simplified clear-sky atmosphere model (Iqbal, 1983) is used to split top-of-the-atmosphere solar irradiance into attenuated direct and diffuse components arriving at the surface.

$$E_{net} + E_{sensible} + E_{latent} + E_{ground} = 0 \qquad (3)$$

The total energy balance at the topographic surface for bare soil is given by Equation 3. The net radiation flux density E_{net} is the sum of all incoming and outgoing radiant flux densities. Sensible heat flux density $E_{sensible}$ is calculated using the bulk aerodynamic method (Formula 4) with the constants air density p_a (kg m^{-3}) and specific heat of air at constant pressure C_a (J kg^{-1} K^{-1}). The driving force of the heat exchange is the temperature gradient between surface and air $T_s - T_a$ (K). The aerodynamic resistance r_a (s m^{-1}) is dependent on wind speed and surface roughness.

$$E_{sensible} = p_a \cdot C_a \cdot \frac{T_s - T_a}{r_a} \qquad (4)$$

Focus has been set on arid desert-like environments thus the latent heat flux density E_{latent} is not modelled and the ground heat flux density E_{ground} is calculated from the subsurface temperature gradient.
The deviation E_{gap} from the energy equilibrium (Formula 3) is used to compute a correction offset for the temperature estimate of the surface layer. Wang & Bras (1999) propose that the ground heat flux density is completely determined by the history of surface soil temperature. In reverse, when given the soil heat flux density E_s, the soil temperature T_g can be calculated. For the surface it leads to Formula 5 with the rock specific volumetric heat conductivity k_s (J m^{-1} s^{-1} K^{-1}) and heat capacity C_s (J m^{-3} K^{-1}).

Assuming that only the deviation E_{gap} from the energy equilibrium can cause a change in surface temperature and that it acts like an additional flux density in the upper layer then solving the integral for the discrete time step [0…t] gives Expression 6.

$$T_g(t) = T_0 + \frac{1}{\sqrt{\pi \cdot k_s C_s}} \int_0^t \frac{E_s}{\sqrt{t-s}} ds \qquad (5)$$

$$T_t = T_{t-1} + \frac{2\sqrt{\Delta t}}{\sqrt{\pi \cdot k_s C_s}} \cdot E_{gap} \qquad (6)$$

The temperature profile in the subsurface was calculated by solving the heat conduction problem in vertical direction by implicit Euler finite differences method (Rosema, 2000) leading to Formula 7. The lower boundary condition is set to a constant temperature assuming no diurnal or annual variations at that depth. For simulating the heat source of a subsurface coal fire this lower boundary condition is set to a higher value. The value of the upper boundary condition is adapted every time step and mimics the diurnal temperature wave.

$$-C_s \cdot \frac{\partial T}{\partial t} = -k_s \cdot \frac{\partial^2 T}{\partial z^2} \qquad (7)$$

$$-C_s \cdot \frac{T_z^t - T_z^{t-1}}{\Delta t} = 2k_s \cdot \frac{\dfrac{T_{z+1}^t}{\Delta z_{z+1}} - \dfrac{T_z^t}{\Delta z_{z+1}} - \dfrac{T_z^t}{\Delta z_z} + \dfrac{T_{z-1}^t}{\Delta z_z}}{\Delta z_z + \Delta z_{z+1}}$$

4. CFRE SIMULATION

The total emitted energy flux (W m^{-2}) over all wavelengths of a grey body with emissivity ε (-) and at temperature T (K) can be calculated according to Formula 8, where σ (W m^{-2} K^{-4}) is the Stefan-Boltzmann constant.

$$E = \varepsilon \cdot \sigma \cdot T^4 \qquad (8)$$

Using Formula 9 the CFRE can be calculated from the difference in total emitted energy flux E of a grey body at coal fire induced surface temperature T_{fire} and a grey body at background/ambient temperature T_{bg} multiplied by the anomaly area A (m^2).

$$CFRE = \left(E(T_{fire}) - E(T_{bg})\right) \cdot A \qquad (9)$$

Feeding the model with the appropriate data a simulation of the surface temperature above a coal fire as well as the site and season specific natural background surface temperature not influenced by the coal fire for any desired time is possible. With the help of Formula (9) a simulated CFRE can be calculated or summed up over a longer period.

5. RESULTS

4.1 ASTER derived CFRE time series
Figure 1 visualizes the temporal development of CFRE derived from the ASTER night time imagery for whole Wuda area and for Wuda fire zone 18 only. First uses at-sensor radiances and a first-order relationship (Zhukov, 2010) latter uses ground-leaving radiances and a second-order relationship (Tetzlaff, 2004).
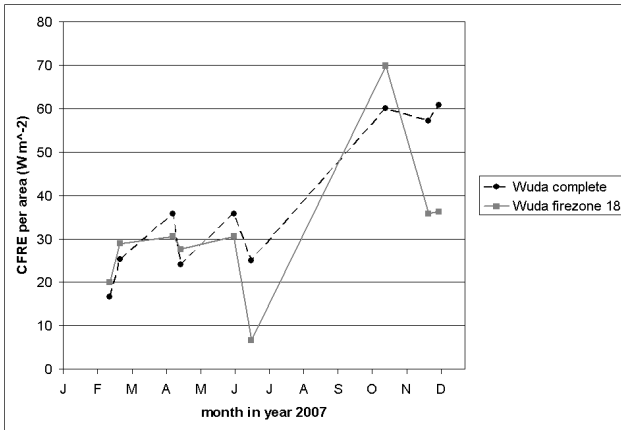
Figure 1. ASTER derived CFRE for whole Wuda area (black circle) and for Wuda fire zone 18 only (gray square).

Noteworthy is the distinct increase in CFRE for the last three scenes (October, November and December 2007) as well as the discrepancy between mean CFRE for whole Wuda area and CFRE for fire zone 18 in mid of June, November and December. The CFRE increase and following discrepancy can be explained by excavating activities in Wuda area exposing formerly covered fires and heated rocks at the surface. The discrepancy mid of June might be explained by differences in atmospheric correction. Zhukov (2010) reports a very high WVC in MODIS data for that scene.

The results of both multi-temporal studies show the feasibility to derive CFRE using ASTER night time images. Due to the coarse spatial resolution of ASTER TIR imagery only few pixels represent a coal fire hence CFRE quantifications are highly dependent on each pixel value. Misclassification of one pixel changes the result significantly. Obviously the detection and quantification result can be improved by a more detailed understanding about the state of the topographic surface in general and especially during satellite overpass. This understanding may be improved by surface energy balance information gained through modelling.

4.2 Simulated temperature profiles

Based on the clear-sky irradiance, topography, climate factors and a subsurface heat source the model calculates the surface temperature considering all major energy balance terms for an arid environment. Attenuation and lag of the diurnal surface temperature wave on its way into deeper soil/rock layers is modelled by incorporating the ground heat flux and thus a link between surface temperature and subsurface temperature at arbitrary depth is established (see Figure 2).

Comparing modelled with measured subsurface temperatures it became obvious that precipitation strongly affects the energy balance. While promoting heat conduction and latent heat flux in a time-variant manner difficult to model, the measured temperature recovered towards the modelled value.

4.3 Simulated CFRE time series

For Wuda fire zone 18 two energy balance models calibrated with the 2008 temperature profile measurements were set up and used to extrapolate surface temperatures in 2007.
The fire influenced surface temperature was calculated for the recording times of the nine ASTER night scenes using the calibrated models. Lacking enough field data the background surface temperature was calculated by setting the subsurface

heat source term of the calibrated model to the 4-year mean air temperature while not changing the model's other parameters. The mean air temperature is averaged from the recordings of four climate stations.
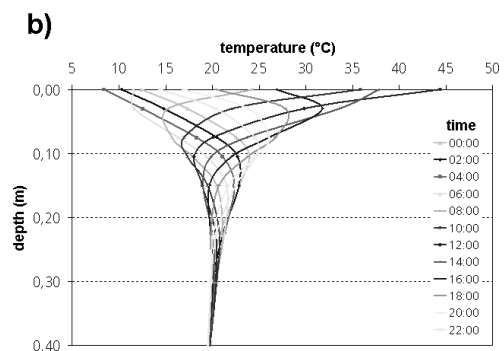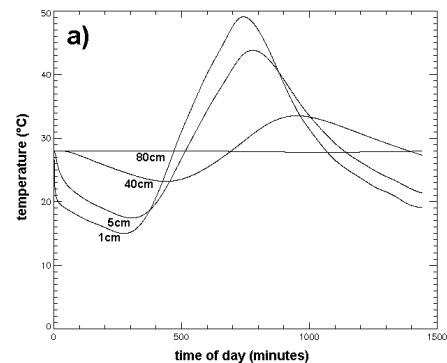

Figure 2. Two examples of modelled soil temperatures for one day. (a) shows the development of soil temperatures at 1cm, 5cm, 20cm and 80cm depth, (b) shows temperature profiles for various times. Damping and phase shift of the diurnal surface temperature wave are clearly visible.

In Figure 3 the ASTER derived CFRE (black squares) for Wuda fire zone 18 is compared to a high temperature model (gray circles) and low temperature model (gray triangles). The high and low temperature model parameters originate from field data acquired during consecutive field trips in 2008 and 2009.
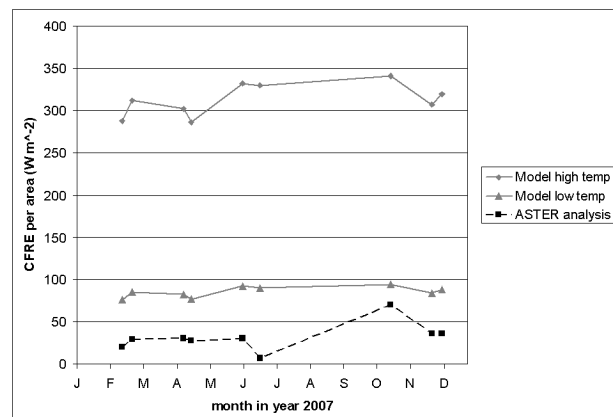

Figure 3. Comparison of modelled CFRE (gray) and ASTER derived (black) CFRE for Wuda fire zone 18.

In general both models show elevated CFRE values compared to the satellite quantifications. Owed to the fact that the models are based on measurements each at a single location above the coal fire, an extrapolation to a whole 90-by-90 m pixel leads to a homogeneous fire pixel with elevated CFRE values compared to a heterogeneous pixel consisting of fire and background as found in the ASTER imagery. The high temperature model represents the situation in a shallow depression near to a small crack exhaling 126 °C hot flue gas. The low temperature model reference location is approximately 100 m southwest on a plateau not shielded from wind.

Taking the ASTER CFRE as reference a sub-pixel fire fraction of 1/10 for the high temperature model (810 m²) and a fraction of 1/3 for the low temperature model (2700 m²) would result in approximately the same total CFRE for a 8100 m² ASTER pixel. Figure 4 shows the remaining discrepancies for the individual scenes. As mentioned above a wrong assumption of WVC for the scene mid of June and excavation activities in October may explain at least partly the deviation peaks.
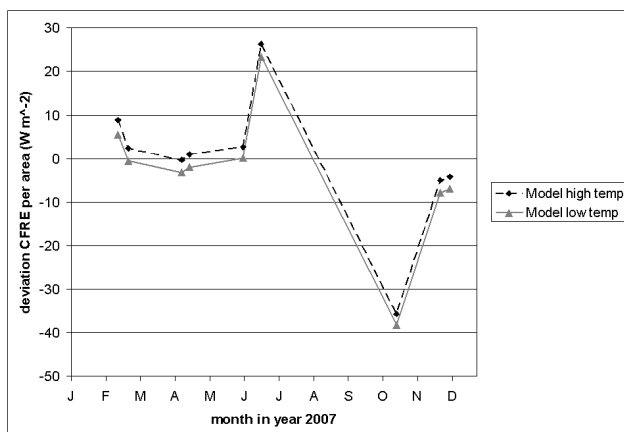

Figure 5. Remaining discrepancy between ASTER derived CFRE and CFRE calculated from high temperature model (black circle) and low temperature model (gray triangle) assuming 1/10 and 1/3 TIR pixel coverage respectively.

6. CONCLUSIONS

The presented model bridges the gap so far existing between coal fire modelling in the subsurface using finite element methods (Rosema, 2000 and Weßling, 2007) and surface temperature measurements (Schlömer, 2010). Focusing on remote sensing, the model can assist to validate land surface temperatures derived from remote sensing data and can serve as background emission value for coal fire radiative energy (CFRE) quantifications. With the ability to simulate hot spot temperatures based on in-situ measurements, verification data can be created to critically review CFRE release computed from satellite data.

The energy balance model at hand gives a coherent description of the atmosphere-surface-subsurface system. However some aspects are missing, namely latent heat flux and heat transport by convection, limiting the model to arid test sites with compact bedrock. Especially climate data with a high temporal resolution are required to model the variable environmental conditions and their influence adequately. If such data is available in future, implementation of these aspects is straightforward.

REFERENCES

Dozier, J., 1981. A method of satellite identification of surface temperature fields of sub-pixel resolution. Remote Sensing of Environment 11: 221-229.

Iqbal, M., 1983. An introduction to solar radiation. New York: Academic Press.

Kaufman, Y.J., Justice, C.O., Flynn, L.P., Kendall, J.D., Prins, E.M., Giglio, L., Ward, D.E., Menzel, W.P., and Setzer, A.W., 1998. Potential global fire monitoring from EOS-MODIS. Journal of Geophysical Research 103: 32215-32238.

Richter, R., 1998. Correction of satellite imagery over mountainous terrain. Applied Optics 37(18).

Rosema, A., Guan, H. and Veld, H., 2000. Simulation of spontaneous combustion, to study the causes of coal fires in the Rujigou Basin. Fuel 80: 7-16

Schlömer, S., 2010. Ground-Based Temperature Measurements Over Subsurface Coal Fires – Lesson Learned and Guidelines. In Proceedings of Second International Conference on Coal Fire Research, Berlin, Germany.

Tetzlaff, A., 2004. Coal fire quantification using ASTER, ETM and BIRD satellite instrument data. Dissertation

Weßling, S., 2007. The investigation of underground coal fires – towards a numerical approach for thermally, hydraulically and chemically coupled processes. Dissertation.

Wooster, M.J., Zhukov, B., and Oertel, D., 2003. Fire radiative energy for quantitative study of biomass burning: derivation from the BIRD experimental satellite and comparison to MODIS fire products. Remote Sensing of Environment 86, 83-107.

Wang, J., Bras, R.L., 1999. Ground heat flux estimated from surface soil temperature. Journal of Hydrology 216: 214-226

Zhang, J., 2004. Spatial and statistical analysis of thermal satellite imagery for extraction of coal fire related anomalies. Dissertation.

Zhukov, B., 2010. Sensor potential evaluation and algorithm development for detection and radiative power evaluation of coal seam fires. In Proceedings of Second International Conference on Coal Fire Research, Berlin, Germany.